Materials Letters 171 (2016) 289–292

Contents lists available at ScienceDirect

Materials Letters

journal homepage: www.elsevier.com/locate/matlet

Titanium doped tin dioxide as potential UV filter with low photocatalytic activity for sunscreen products

Alexander Morlando [a], Dean Cardillo [a], Thierry Devers [b], Konstantin Konstantinov [a,*]

[a] Institute for Superconducting and Electronic Materials, AIIM Facility, University of Wollongong Innovation Campus, Squires Way, North Wollongong, NSW 2500, Australia

[b] Interface, Confinement, Matériaux et Nanostructures – ICMN UMR737, Site IUT de Chartres, France

ARTICLE INFO

Article history:
Received 28 September 2015
Received in revised form
4 February 2016
Accepted 21 February 2016
Available online 23 February 2016

Keywords:
Optical materials and properties
Particles
Nanosize
Powder technology
X-ray techniques

ABSTRACT

Titanium doped tin dioxide nanopowders were produced using a simple precipitation method and displayed the same crystalline structure and decreasing particle size with increasing dopant concentration. Optical absorption studies showed broad absorption in the UV region for each sample and enhanced absorption relative to commercial zinc oxide (ZnO) but significantly less absorption than the uncoated commercial titanium dioxide nanopowder (P-25). Photocatalytic studies showed that the 5%Ti doped sample had the lowest methylene blue (MB) degradation rate of $(1.9 \pm 0.4) \times 10^{-3}$ min^{-1}, followed by the undoped ($(2.6 \pm 0.4) \times 10^{-3}$ min^{-1}) and 10% Ti-doped ($(4.5 \pm 0.4) \times 10^{-3}$ min^{-1}) samples. All of the nanoparticle samples demonstrated substantially lowered photocatalytic activity compared to commercial ZnO and P-25 reference particles.

1. Introduction

Exposure to solar UV radiation is a known cause of many types of skin cancer. In particular, UVA (320–400 nm) and UVB (290–320 nm) radiation have been proven to cause DNA damage both directly and indirectly via the production of reactive oxygen species that bring about oxidative stress [1]. Application of sunscreens containing UV filtering additives (both organic and inorganic) to the skin is a common measure for protecting against UV radiation. Although there are a greater number of certified organic filters than inorganic, these materials typically have a lower photostability, are potential allergens and provide a relatively low level of protection when used on their own. Modern sunscreen formulations now contain a mixture of UV filters and the use of inorganic filters has become more extensive due to their lower potential of producing irritant reactions, high sun protection factor (SPF) and broad-spectrum absorption [2]. Titanium dioxide (TiO_2) and zinc oxide (ZnO) are the aforementioned inorganic filters currently used in sunscreens. Although both materials exhibit high photocatalytic properties which could lead to the production of harmful reactive oxygen species, their broadband absorption across the UVA and UVB range, have led to their extensive use in sunscreen products. Despite the apparent benefits of these nanomaterials, recent concern over the skin penetrating capabilities and potential toxicity has led to further investigation of the safety of these materials. As of 2013, in a review of the safety of TiO_2 and ZnO nanoparticles in sunscreens [3], the weight of evidence suggests that these materials remain on the skin surface and outer layer of the stratum corneum, which is composed only of non-viable cells. However, the review also highlighted the fact that there is conclusive *in vitro* evidence that, whilst in the presence of UV radiation, these materials bring about the production of reactive oxygen species, which can lead to the damaging of cells. As such, it is necessary to search for alternate materials that provide the same, if not improved, benefits provided by TiO_2 and ZnO as UV filters but without potential toxicological effects. Materials based on tin dioxide are most commonly used as transparent conducting oxides, oxidation catalysts and as solid state gas sensing materials [4–6]. With a wide band gap (3.60 eV) [7], tin dioxide has a high optical transparency in the visible light range, making it a potentially cosmetically viable material. Additionally, tailoring of the band gap through induced defect sites and/or impurities could shift its absorption profile into the UVB or UVA range, allowing it to behave as a UV filter. Studies on tin oxide doping with a variety of materials [8–11] have shown that such bandgap tailoring is possible. In this study, the optical and photocatalytic properties of titanium doped tin dioxide nanoparticles prepared via a chemical co-precipitation synthesis method are explored.

* Corresponding author.
E-mail address: konstan@uow.edu.au (K. Konstantinov).

http://dx.doi.org/10.1016/j.matlet.2016.02.094
0167-577X/

2. Experimental

Firstly, 0.2 mol/L solutions of tin(II) chloride ($SnCl_2$, Sigma-Aldrich 98%) and titanium(IV) butoxide ($Ti(OCH_2CH_2CH_2CH_3)_4$, Sigma-Aldrich 97%) were prepared in ethanol. These two solutions were then added to a reaction beaker in quantities for the desired level of Ti-doping (%Ti=0;5;10). While under magnetic stirring, approximately 30 mL of 2 mol/L ammonium hydroxide (NH_4OH, Sigma-Aldrich 28.0 – 30.0% NH_3 basis) was added dropwise to the solution. This resulted in the precipitation of a yellow slurry which was left to stir for an additional 30 min before being removed by centrifugation and subsequently washed several times with distilled water and ethanol. The washed precipitant was then dried in an oven at 90 °C for 12 h, crushed into a powder using a mortar and pestle and calcined in a tube furnace at 500 °C for 5 h to obtain the final $Ti_xSn_{1-x}O_2$ product.

The crystalline phase and mean crystallite sizes for the pure and Ti-doped tin oxide samples were analysed by XRD using a GBC MMA x-ray diffractometer. Further particle size analysis was performed from TEM micrographs obtained using a JEOL ARM200F Transmission Electron Microscope. UV–vis absorption and diffuse reflectance spectra were collected using a Shimadzu UV 3600 UV–vis-NIR spectrophotometer in the scan range of λ 200 – 1000 nm. Samples were initially dispersed in ethanol to a concentration of 0.05 gL^{-1} via sonication for an hour before the absorption measurements were made. Dry powder samples were spread between quartz microscope slides, ensuring an even consistency in the spread of the material before being diffuse reflectance measuring.

The photocatalytic activity was evaluated by the decomposition of an aqueous 100 mg/L methylene blue (MB) (Sigma-Aldrich, ≥ 95%) solution in presence of powder sample. A Rayonet photocatalytic reactor lined alternatingly with 350 nm and 300 nm phosphor-coated lamps was used as the irradiation source. Typically, 25 mg of powder photocatalyst was added to 25 mL of MB and the mixture left to stir in darkness for an hour so as to establish the absorption-desorption equilibrium between the photocatalyst and the dye [11]. During irradiation, 3 mL aliquots from the reaction mixture were collected periodically over the course of an hour and diluted to 30 mL in deionized water. The powders were removed by centrifugation and the resultant degradation was determined by measuring the major peak absorbance for methylene blue at λ=664 nm using a Shimadzu UV 1800 UV–vis-NIR spectrometer. Comparison studies with commercial ZnO and P-25 were also conducted.

3. Results and discussion

Fig. 1 highlights the XRD patterns of the as-prepared powder samples. Each sample XRD pattern was indexed to the tetragonal rutile phase of tin dioxide (JCPDS 01-071-0652). No significant peak shifting with increasing Ti dopant concentration was observed, however, peak broadening and a lowering of peak intensities did occur in accordance with decreasing crystallite sizes. Calculation of the mean crystallite size using the Scherrer formula was confirmed with crystallite size analysis from the TEM micrographs obtained (Table 1). The reduction of crystallite size with increasing dopant concentration suggests an inhibition of crystallite growth due to a reduction in the grain boundary mobility, which has been reported for SnO_2 with various other dopants [8,12,13]. Lattice parameters for each sample were calculated using the Rietveld refinement extension program for the Materials Analysis Using Diffraction (MAUD) software. The decrease in lattice parameters correlates with the slight shifts in the XRD peak positions with increasing dopant concentration towards higher diffraction angles and is consistent with the substitution of the

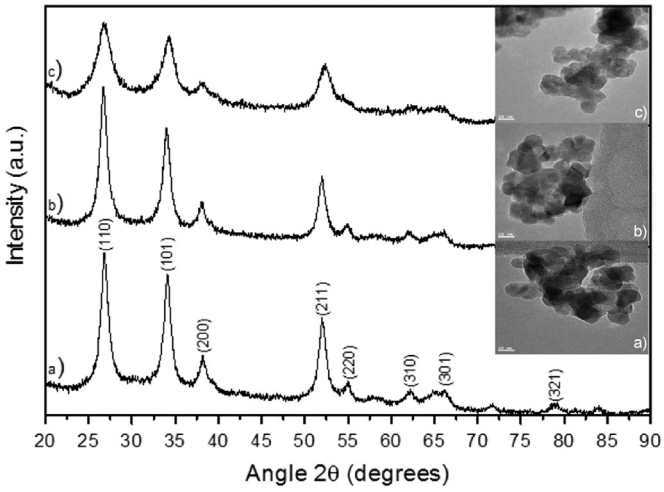

Fig. 1. XRD patterns with (*h k l*) indices and accompanying TEM images for a) SnO_2, b) $Ti_{0.05}Sn_{0.95}O_2$ and c) $Ti_{0.10}Sn_{0.90}O_2$ powder samples.

larger ionic radii Sn^{4+} ions by the smaller Ti^{4+} ions (0.071 nm and 0.068 nm respectively) [14]. Samples displayed a combination of spheroidal and granular crystallite morphologies as highlighted in Fig. 1. Additionally, agglomeration of the smaller crystallites is apparent, resulting in the formation of larger secondary particles.

The absorption spectra (Fig. 2) of the as-prepared samples all exhibit major absorption between wavelengths (λ) 270–315 nm (UVC, UVB region). Considerable absorption for each sample in the region of 400–600 nm is evident, resulting in an opaque appearance of samples when in solution. Such absorption features have been reported in nanocrystalline SnO_2 calcined in vacuum at various temperatures and has been attributed to the presence of neutral oxygen vacancies and isolated Sn^{2+} ions [15]. Such features in semi-conductor nanomaterials are referred to as Urbach tails and indicate the presence of impurity states outside the bandgap region [16]. Optical band gaps for each sample were calculated from their diffuse reflectance spectra and subsequent conversion to absorption coefficient (α) values. In accordance with the Tauc relation, plots of $(\alpha h\nu)^n$ against $h\nu$ yield an estimation of the band gap by extrapolation of the curve to the x-axis, where $h\nu$ is the photon energy and n the nature of the transition between the valence and conduction bands in the material. SnO_2 is reported to have a direct allowed band gap transition [17] and so a value of 2 was used in place of *n*. A comparison of the band gap energies with the mean crystallite sizes for each sample show that the band gap increases with decreasing crystallite size, along with increasing concentration of dopant atoms. This trend may be attributed to the three dimensional quantum confinement effect observed in semiconducting nanoparticles, whereby, as the particle approaches the materials excitonic Bohr radius, it exhibits a blue shift in band gap energy. In our case, the particle sizes are larger than that of the Bohr radius of SnO_2 [12,18], and so, other factors, such as lattice strain, doping concentration and surface effects contribute more prominently [12]. Although the as-prepared samples display greater absorption properties than the ZnO (Fig. 2) tested, the absorption bands for each sample lie outside of the desired UVA region, however, the considerable absorption still observed in this region highlights the potential of the as-prepared samples for use as potential broad spectrum filters.

The photocatalytic activity of the as-prepared powder samples, as well as the commercial ZnO and P-25 for comparison, were evaluated by measuring the degradation of MB under UV irradiation over a period of 60 min. The degradation of dyes has been previously ascribed to a pseudo-first-order reaction using the Langmuir-Hinshelwood model [15]. The expression for the